Olfactory neuronal cells: biopsied surrogates for neurons in the brain

Kun Yang[1], Koko Ishizuka[1], Zui Narita[1], Yukiko Y. Lema[1], Siwei Zhang[9], Jubao Duan[9,10], Laurent Younes[8], Donald Geman[8], Andy Lane[6], Akira Sawa[1,2,3,4,5,7,*]

Departments of Psychiatry[1], Biomedical Engineering[2], Neuroscience[3], Phamarchology[4], Genetic Medicine[5], and Otolaryngology-Head and Neck Surgery[6]

Johns Hopkins University School of Medicine, Baltimore, Maryland.

Departments of Mental Health[7],

Johns Hopkins Bloomberg School of Public Health, Baltimore, Maryland.

Department of Applied Math and Statistics[8],

Johns Hopkins University Whiting School of Engineering, Baltimore, MD 21218, USA

Center for Psychiatric Genetics[9],

NorthShore University HealthSystem, Evanston, IL 60201, USA

Department of Psychiatry and Behavioral Neuroscience[10],

University of Chicago, Chicago, IL 60637, USA

[*]Corresponding author: asawa1@jhmi.edu

ABSTRACT

Biopsy is an essential procedure of clinical medicine in which we obtain tissues and cells that are supposed to directly reflect pathological changes of each disease. Biopsy from the brain is difficult at both practical and ethical levels. Nasal biopsy that captures tissues with olfactory neurons has been considered as an alternative method of obtaining neurons from living patients with brain disorders. However, insufficient characterization of biopsied cells/tissues has hampered a wider use of nasal tissues as surrogate resources for the brain. By conducting single cell and bulk RNA-sequence analysis of olfactory neuronal cells (ONCs) enriched from nasal biopsied tissues and using multiple pubic datasets in comparison, we now report precise characterization of ONCs at the molecular levels. These cells are easily and reproducibly prepared and have two major strengths. They are homogeneous and neuronal, resembling excitatory neurons in the dorsolateral prefrontal cortex and anterior cingulate cortex in molecular signatures.

INTRODUCTION

Biopsy is an essential procedure of clinical medicine in which we obtain tissues and cells that are supposed to directly reflect pathological changes of each disease. Biopsy from the brain is difficult at both practical and ethical levels. Nasal biopsy that captures tissues with olfactory neurons has been considered as an alternative method of obtaining neurons from living patients with brain disorders. Nevertheless, insufficient characterization of biopsied cells/tissues has hampered a wider use of nasal tissues as surrogate resources for the brain.

We recently suggested the potential utility of olfactory neuronal cells (ONCs) enriched from nasal biopsied tissues for brain disease research. However, these cells were not characterized by the frontline molecular methodology. By conducting single cell and bulk RNA-sequence analysis of ONCs and using multiple pubic datasets in comparison, we now report the precise characterization of ONCs at the molecular levels.

METHODS

Study participants

To demonstrate the validity and utility of ONCs as surrogate neuronal cells, in the present study, we used clinical data and biospecimens collected from study participants recruited by clinical cohorts[1–16] established at Johns Hopkins Schizophrenia Center under approval of the Johns Hopkins Medicine Institutional Review Boards. All study participants provided written informed consent. All study participants have no history of traumatic brain injury, cancer, abnormal bleeding, and other major physical conditions, no drug or alcohol abuse in the past three years, and no illicit drug use in the past two months. Healthy controls have no personal or immediate

family history of psychosis without current psychotropic medication. Patients received the Structured Clinical Interview for DSM-IV (SCID-IV) by study team psychiatrists. Patients with chronic schizophrenia or first episode psychosis (disease onset within 24 months at the first study enrollment) were used in this study. Collateral information for patients was also gathered from available medical records.

Nasal biopsy

Nasal biopsy was performed under endoscopic control with local anesthesia to the nasal cavity provided by lidocaine liquid 4% and oxymetazoline HCl 0.05% spray, followed by injection of 1% lidocaine and 1/100,000 epinephrine. OE is more likely to be found further back in the nasal cavity on the septum as well as on the turbinates[17]. More specifically, the probability of obtaining OE was reportedly 40 %, 76 %, 30-50 %, 73 %, and 58 % at the dorsomedial and the dorsoposterior areas of the septum, the dorsomedial and dorsoposterior areas of the superior turbinate, and the middle turbinate, respectively[17]. Based on this information, three tissue pieces were taken from the OE regions of the septum from each nostril (total 6 pieces) by using an ethmoid forceps by avoiding trauma to the cribriform plate. When accessing to the septum was difficult, the superior turbinate was targeted. After the biopsy, participants were observed in the clinic for 15 to 30 min with no packing or treatment. One participant claimed bleeding and was treated with packing among more than 400 biopsies so far.

ONCs

Figure S1 summarizes the procedure of enriching ONCs from nasal biopsy. First, biopsied tissues were incubated with 2.4 U/mL Dispase II for 45 min at 37ºC, and mechanically minced

into small pieces. Then, the tissue pieces were further treated with 0.25 mg/mL collagenase A for 10 min at 37ºC. Dissociated cells were gently suspended, and centrifuged to obtain pellets. Cell pellets were resuspended in DMEM/F12 supplemented with 10% FBS and antibiotics (D-MEM/F12 medium) and tissue debris was removed by transferring only the cell suspension into a new tube. Cells from the suspension were then plated on 6-well plates in fresh D-MEM/F12 medium (Day 0 plate). Cells floating were collected at days 2 (Day 2 plate) and day 7 (Day 7 plate), and further incubated on 6-well plates. Through these processes, connective tissue-origin cells and non-neuronal cells that are attached in Day 0 and 2 plates were removed. Accordingly, in the present study, we examined cells in Day 7 plate called ONCs under the hypothesis that these are neuronal and homogeneous. ONCs were aliquoted and stored in liquid nitrogen tanks until further experiments, in which ONCs were recovered and cultured in the D-MEM/F12 medium with the media change every 2-3 days.

External datasets

Datasets used as references in the study of the homogeneity of ONCs:

(1) HEK293T and Jurkat cells[18].

(2) Human embryonic stem cell (hESC) and hESC-derived neurons after 26 and 54 days' of induction[19].

(3) Human induced pluripotent stem cell (hiPSC)-derived cerebral organoid[20].

(4) Mouse brain (10X chromium demonstration dataset: https://support.10xgenomics.com/single-cell-gene-expression/datasets/2.1.0/neurons_2000).

Datasets used as references in the study of the neuronal characteristics of ONCs:

(1) single-nucleus RNA sequencing (snRNA-seq) from postmortem dorsolateral prefrontal cortex, subgenual anterior cingulate cortex, hippocampus, nucleus accumbens, and amygdala of normal donors published by Tran et al[21].

(2) snRNA-seq from postmortem prefrontal cortex of normal donors published by Velmeshev et al[22].

(3) snRNA-seq from postmortem middle temporal gyrus of normal donors published by Hodge et al[23].

(4) Bulk RNA-Seq from postmortem brains at difference developmental stages (fetus, infancy, childhood, adolescence, and adulthood) released by BrainSpan[24].

(5) Bulk RNA-seq from iPSC-derived neural progenitor cells, mature neurons, and microglia collected by researchers of this project (SZ and JD).

Datasets used as quality controls for *Seurat* cell type prediction:

(1) Neurons isolated by using neuronal nuclear antigen (NeuN) from the postmortem brain of normal donors[25].

(2) hESC-derived neurons after 54 days' of induction[19].

(3) Microglia isolated by FACS sorting from postmortem brains of normal donors[26].

Bulk RNA-Seq

Total RNA was isolated from the ONCs using the RNeasy Plus Mini Kit (Qiagen). The quality of RNA was assessed via Agilent Fragment Analyzer analysis using an RNA High Sensitivity (DNF-472) and quantified using a Qubit 4 RNA BR kit (Thermo Fisher). RNA libraries were prepared with 500ng total RNA. Library generation was accomplished using NEBNext Ultra II

Directional RNA Library Prep Kit for Illumina (E7760 and E7490) following the NEBNext Poly(A) mRNA Magnetic Isolation Module protocol. Libraries were enriched using 11 cycles of PCR amplification. Library quality and quantification was assessed via Fragment Analyzer analysis using a High Sensitivity NGS Kit (DNF-474) and Qubit 4. Samples were then normalized to 4nM and pooled in equimolar amounts. Paired-End Sequencing was performed using Illumina's NovaSeq6000 S4 200 cycle kit.

FastQC[27] was used to check the quality of reads. High quality data were obtained from raw data by using cutadapt[28] to remove adapters, primers, and reads with low quality (option -q 10) or shorter than 20 nt. *Hisat2*[29] (option --dta) was used to map the clean reads to the human genome, version GRCh38 (Genome Reference Consortium Human Build 38). *Stringtie*[29] was used to assemble and merge transcripts and estimate transcript abundances. A Python script (prepDE.py) provided by *Stringtie* developer[29] was used to create count tables. *Combat*[30] was used to adjust the batch effects. The processed bulk RNA-Seq data from healthy controls were used to study the neuronal characteristics of ONCs via UMAP (Uniform Manifold Approximation and Projection)[31].

scRNA-Seq

scRNA-seq was performed by the 10xGenomic single cell 3′ library platform. Briefly, single cells were sorted into 1.5 mL tubes (Eppendorf) and counted under the microscope. Cells were loaded at 10,000-100,000 cells/chip position using the Chromium Single cell 3′ Library, Gel Bead & Multiplex Kit and Chip Kit (10× Genomics, V2 barcoding chemistry) and the subsequent steps were performed according to the manufacturer’s instructions. Purified libraries

were analyzed by an Illumina NovaSeq sequencer. Cell Ranger[18] was used to check the quality of raw sequencing data, map reads to human genome hg19[32], and create count tables for downstream analysis.

The processed scRNA-Seq data were used to study the homogeneity of ONCs via UMAP and intercorrelation analysis of each sample (each cell type or tissue). The intercorrelation analysis was conducted as follows:

(1) Select 2000 genes with the highest variance across all the cells in the sample based on a variance stabilizing transformation (*Seurat vst* method[33,34]).

(2) Calculate the Spearman correlation of those 2000 genes between two cells in the sample. Cells were randomly paired and the correlations of 10,000 pairs were calculated.

(3) Calculate the mean correlation coefficients and standard deviation, and adjust the batch effect caused by different sequencing platforms. The mean correlation coefficients were used to evaluate the homogeneity. Samples with larger mean correlation coefficients are more homogeneous.

The processed scRNA-Seq data were also used to study the neuronal characteristics of ONCs via UMAP and *Seurat* cell type prediction. *Seurat* cell type prediction was conducted as follows:

(1) Preparation of testing and training datasets: calculate unique molecular identifiers per million reads (UPM); remove genes with low expressional levels (mean UPM smaller than 0.1); log transform UPMs for further analysis.

(2) Identification of variable features: run *Seurat FindVariableFeatures* function with parameters *selection.method = "vst"* and *nfeatures = 2000*.

(3) Identification of anchors: run *Seurat FindTransferAnchors* function with parameter *dims = 1:30*.

(4) Prediction of cell types: run *Seurat TransferData* function with parameters *dims = 1:30* and *k.weight=10*

(5) Quality control: publicly available datasets from known cell types were used to verify that the above steps can produce correct predictions.

RESULTS AND DISCUSSIONS

We recently suggested the potential utility of olfactory neuronal cells (ONCs) enriched from nasal biopsied tissues for brain disease research (**Figure S1**). One of the major goals of the present study is to establish a precise characterization of ONCs at the molecular level by using frontline next-generation sequencing techniques.

ONCs are homogeneous

First, we addressed whether and how much ONCs are homogeneous. To address this question, we compared scRNA-Seq data from ONCs of three healthy controls (**Table S1**) with scRNA-Seq data from immortalized cell lines (HEK293T and Jurkat cells), hESC-derived neurons after 26 and 54 days' of induction[19], hiPSC-derived cerebral organoid, and mouse brain, respectively.

Intercorrelation analysis with scRNA-seq data found that ONCs had similar homogeneity as well-established homogeneous cell lines like HEK293T and Jurkat cells (**Figure 1A**). The mean correlation coefficients between cell pairs of each ONC samples were 0.57, 0.60, and 0.62, while the mean correlation coefficient of both HEK293T and Jurkat cells was 0.65. On the other hand,

hESC-derived cells were more heterogeneous, where the mean correlation coefficients of hESC-derived neuronal progenitors after 26 days' differentiation and after 54 days' differentiation were 0.54. and 0.42, respectively. For iPSC-derived cortical organoid and brain tissue with heterogeneous cell populations, the mean correlation coefficients were 0.49 and 0.44, respectively.

Furthermore, we created UMAP plots to visualize the homogeneity characteristics of ONCs. Similar to Jurat, ONCs were gathered in one cluster (**Figure 1B, C**), while brain tissue and hESC-derived neurons after 54 days' induction were scattered into sub-clusters (**Figure 1D, E**). Together, these results suggested that ONCs were close to homogeneous cell lines and were much more homogeneous than hESC/hiPSC-derived neurons or organoids.

ONCs have similar molecular profiles as neurons

Next, we addressed whether and how much ONCs are neuronal in the molecular signature. To address this question, we compared bulk RNA-Seq and scRNA-Seq data from ONCs with those from the brains, hiPSC-derived neuronal cells, and olfactory tissues.

We conducted UMAP analysis using bulk RNA-Seq data from ONCs of 61 healthy controls (**Table S2**) and bulk RNA-Seq data from multiple publicly available datasets as references. Our analysis showed that ONCs were most similar to the fetal brain compared with brains at other developmental stages (infancy, childhood, adolescence, and adulthood) (**Figure S2A**). Compared with iPSC-derived cells, ONCs were most similar to neuronal progenitors, close to mature neurons, and different from microglia (**Figure S2B**).

We also utilized scRNA-Seq data from ONCs of 3 healthy controls (**Table S1**) and snRNA-Seq data from publicly-available postmortem brain datasets as references (three independent datasets, see Methods "**External datasets**" section). *Seurat* predicted ONCs as neurons against other cell types in the brain including astrocytes, microglia, oligodendrocytes, oligodendrocyte progenitor cells, and endothelial cells, for all the three reference datasets (**Figure 2A, 2B**; **Figure S3**).

When comparing ONCs with neuronal subtypes from five different brain regions [the dorsolateral prefrontal cortex (DLPFC), subgenual anterior cingulate cortex (sACC), hippocampus, nucleus accumbens, and amygdala] reported by Tran et al[21], *Seurat* predicted the majority of ONCs as excitatory neurons in DLPFC and sACC (**Figure 2C**). UMAP analysis also confirmed these results (**Figure 2D, 2E**).

Lastly, we compared scRNA-Seq data from ONCs with those from the olfactory tissues[35]. UMAP analysis found that ONCs were the most similar to horizontal basal cells and were different from pericytes and fibroblasts (**Figure S4**). Olfactory horizontal basal cells are stem cells that could regenerate olfactory neurons and non-neuronal cells when injuries happened[36].

Together, our study showed that ONCs are homogeneous neuronal cells, which may be a useful cell resource for studying molecular signatures of brain disorders.

Acknowledgments:

This study is supported by National Institutes of Mental Health Grants MH-092443 (to AS), MH-094268 (to AS), MH-105660 (to AS), and MH-107730 (to AS); foundation grants from Stanley (to AS), RUSK/S-R (to AS), a NARSAD young investigator award from Brain and Behavior Research Foundation (to AS, KY), DC-016106 (to AL), and AI-132590 (to AL). The authors thank Dr. Lin for conducting the nasal biopsy and appreciate Yukiko Lema for research management and manuscript organization.

References

1. Kano, S. *et al.* Genome-wide profiling of multiple histone methylations in olfactory cells: further implications for cellular susceptibility to oxidative stress in schizophrenia. *Mol. Psychiatry* **18**, 740–742 (2013).
2. Etyemez, S. *et al.* Olfactory dysfunction and face processing of social cognition in first-episode psychosis. *Neurosci Res* S0168-0102(21)00211-X (2021) doi:10.1016/j.neures.2021.10.003.
3. Etyemez, S. *et al.* Brain regions associated with olfactory dysfunction in first episode psychosis patients. *World J Biol Psychiatry* 1–9 (2022) doi:10.1080/15622975.2022.2082526.
4. Kamath, V. *et al.* Contributions of olfactory and neuropsychological assessment to the diagnosis of first-episode schizophrenia. *Neuropsychology* **33**, 203–211 (2019).
5. Kamath, V., Lasutschinkow, P., Ishizuka, K. & Sawa, A. Olfactory Functioning in First-Episode Psychosis. *Schizophr Bull* **44**, 672–680 (2018).
6. Mor, E. *et al.* MicroRNA-382 expression is elevated in the olfactory neuroepithelium of schizophrenia patients. *Neurobiol Dis* **55**, 1–10 (2013).
7. Yang, K. *et al.* Volumetric alteration of olfactory bulb and immune-related molecular changes in olfactory epithelium in first episode psychosis patients. *Schizophr Res* **235**, 9–11 (2021).
8. Posporelis, S. *et al.* Decoupling of Brain Temperature and Glutamate in Recent Onset of Schizophrenia: A 7T Proton Magnetic Resonance Spectroscopy Study. *Biol Psychiatry Cogn Neurosci Neuroimaging* **3**, 248–254 (2018).
9. Coughlin, J. M. *et al.* A multimodal approach to studying the relationship between peripheral glutathione, brain glutamate, and cognition in health and in schizophrenia. *Mol Psychiatry* **26**, 3502–3511 (2021).

10. Wang, A. M. *et al.* Assessing Brain Metabolism With 7-T Proton Magnetic Resonance Spectroscopy in Patients With First-Episode Psychosis. *JAMA Psychiatry* **76**, 314–323 (2019).

11. Yang, K. *et al.* A multimodal study of a first episode psychosis cohort: potential markers of antipsychotic treatment resistance. *Mol Psychiatry* **27**, 1184–1191 (2022).

12. Faria, A. V. *et al.* Relationship between neuropsychological behavior and brain white matter in first-episode psychosis. *Schizophr. Res.* **208**, 49–54 (2019).

13. Faria, A. V. *et al.* Multimodal MRI assessment for first episode psychosis: A major change in the thalamus and an efficient stratification of a subgroup. *Hum Brain Mapp* **42**, 1034–1053 (2021).

14. Narita, Z. *et al.* Face processing of social cognition in patients with first episode psychosis: Its deficits and association with the right subcallosal anterior cingulate cortex. *Schizophr Res* **238**, 99–107 (2021).

15. Nucifora, L. G. *et al.* Increased Protein Insolubility in Brains From a Subset of Patients With Schizophrenia. *AJP* **176**, 730–743 (2019).

16. Avigdor, B. E. *et al.* Characterization of antipsychotic medications, amino acid signatures, and platelet-activating factor in first-episode psychosis. *Biomarkers in Neuropsychiatry* **5**, 100045 (2021).

17. Féron, F., Perry, C., McGrath, J. J. & Mackay-Sim, A. New techniques for biopsy and culture of human olfactory epithelial neurons. *Arch Otolaryngol Head Neck Surg* **124**, 861–866 (1998).

18. Zheng, G. X. Y. *et al.* Massively parallel digital transcriptional profiling of single cells. *Nat Commun* **8**, 14049 (2017).

19. Yao, Z. *et al.* A single cell roadmap of lineage bifurcation in human ESC models of embryonic brain development. *Cell Stem Cell* **20**, 120–134 (2017).

20. Camp, J. G. *et al.* Human cerebral organoids recapitulate gene expression programs of fetal neocortex development. *PNAS* **112**, 15672–15677 (2015).

21. Tran, M. N. *et al.* Single-nucleus transcriptome analysis reveals cell-type-specific molecular signatures across reward circuitry in the human brain. *Neuron* **109**, 3088-3103.e5 (2021).

22. Velmeshev, D. *et al.* Single-cell genomics identifies cell type–specific molecular changes in autism. *Science* **364**, 685–689 (2019).

23. Hodge, R. D. *et al.* Conserved cell types with divergent features in human versus mouse cortex. *Nature* **573**, 61–68 (2019).

24. Miller, J. A. *et al.* Transcriptional landscape of the prenatal human brain. *Nature* **508**, 199–206 (2014).

25. Lake, B. B. *et al.* Neuronal subtypes and diversity revealed by single-nucleus RNA sequencing of the human brain. *Science* **352**, 1586–1590 (2016).

26. Gerrits, E., Heng, Y., Boddeke, E. W. G. M. & Eggen, B. J. L. Transcriptional profiling of microglia; current state of the art and future perspectives. *Glia* **68**, 740–755 (2020).

27. Andrews, S. FastQC: a quality control tool for high throughput sequence data. (2010).

28. Martin, M. Cutadapt removes adapter sequences from high-throughput sequencing reads. *EMBnet.journal* **17**, 10–12 (2011).

29. Pertea, M., Kim, D., Pertea, G. M., Leek, J. T. & Salzberg, S. L. Transcript-level expression analysis of RNA-seq experiments with HISAT, StringTie and Ballgown. *Nat Protoc* **11**, 1650–1667 (2016).

30. Leek, J. T., Johnson, W. E., Parker, H. S., Jaffe, A. E. & Storey, J. D. The sva package for removing batch effects and other unwanted variation in high-throughput experiments. *Bioinformatics* **28**, 882–883 (2012).

31. McInnes, L., Healy, J., Saul, N. & Großberger, L. UMAP: Uniform Manifold Approximation and Projection. *J. Open Source Softw.* **3**, 861 (2018).

32. Haeussler, M. *et al.* The UCSC Genome Browser database: 2019 update. *Nucleic Acids Res* **47**, D853–D858 (2019).

33. Butler, A., Hoffman, P., Smibert, P., Papalexi, E. & Satija, R. Integrating single-cell transcriptomic data across different conditions, technologies, and species. *Nat Biotechnol* **36**, 411–420 (2018).

34. Stuart, T. *et al.* Comprehensive Integration of Single-Cell Data. *Cell* **177**, 1888-1902.e21 (2019).

35. Durante, M. A. *et al.* Single-cell analysis of olfactory neurogenesis and differentiation in adult humans. *Nat. Neurosci.* **23**, 323–326 (2020).

36. Iwai, N., Zhou, Z., Roop, D. R. & Behringer, R. R. Horizontal Basal Cells Are Multipotent Progenitors in Normal and Injured Adult Olfactory Epithelium. *Stem Cells* **26**, 1298–1306 (2008).

Figure legend

Figure 1. Comparison of single-cell RNA sequencing (scRNA-Seq) data between olfactory neuronal cells (ONCs) and homogeneous/heterogeneous cell populations.

A) Intercorrelation analysis results

B) UMAP visualizations of Jurkat cells

C) UMAP visualizations of ONCs

D) UMAP visualizations of the brain tissue

E) UMAP visualizations of hESC-derived neurons after 54 days of induction.

Figure 2. Comparison of single-cell RNA sequencing (scRNA-Seq) data between olfactory neuronal cells (ONCs) and human brain cells.

A) *Seurat* predictions of the cell type of ONCs against human brain cell types in postmortem dorsal prefrontal cortex (DLPFC). Labels on the left side of the heatmap are for reference cell types, while labels on the bottom of the heatmap are for tested cell types. The prediction score indicates how confident *Seurat* is in making the call.

B) *Seurat* predictions of the cell type of ONCs against human brain cell types in subgenual anterior cingulate cortex (sACC).

C) *Seurat* predictions of the cell type of ONCs against neuron subtypes across 5 different brain regions: DLPFC, sACC, hippocampus (HP), nucleus accumbens (NAc), and amygdala (Amyg).

D) UMAP visualization of ONCs projected on the 2D space of neuron subtypes in five brain regions.

E) UMAP visualization of ONCs projected on the 2D space of brain cells in sACC.

Figure 1.

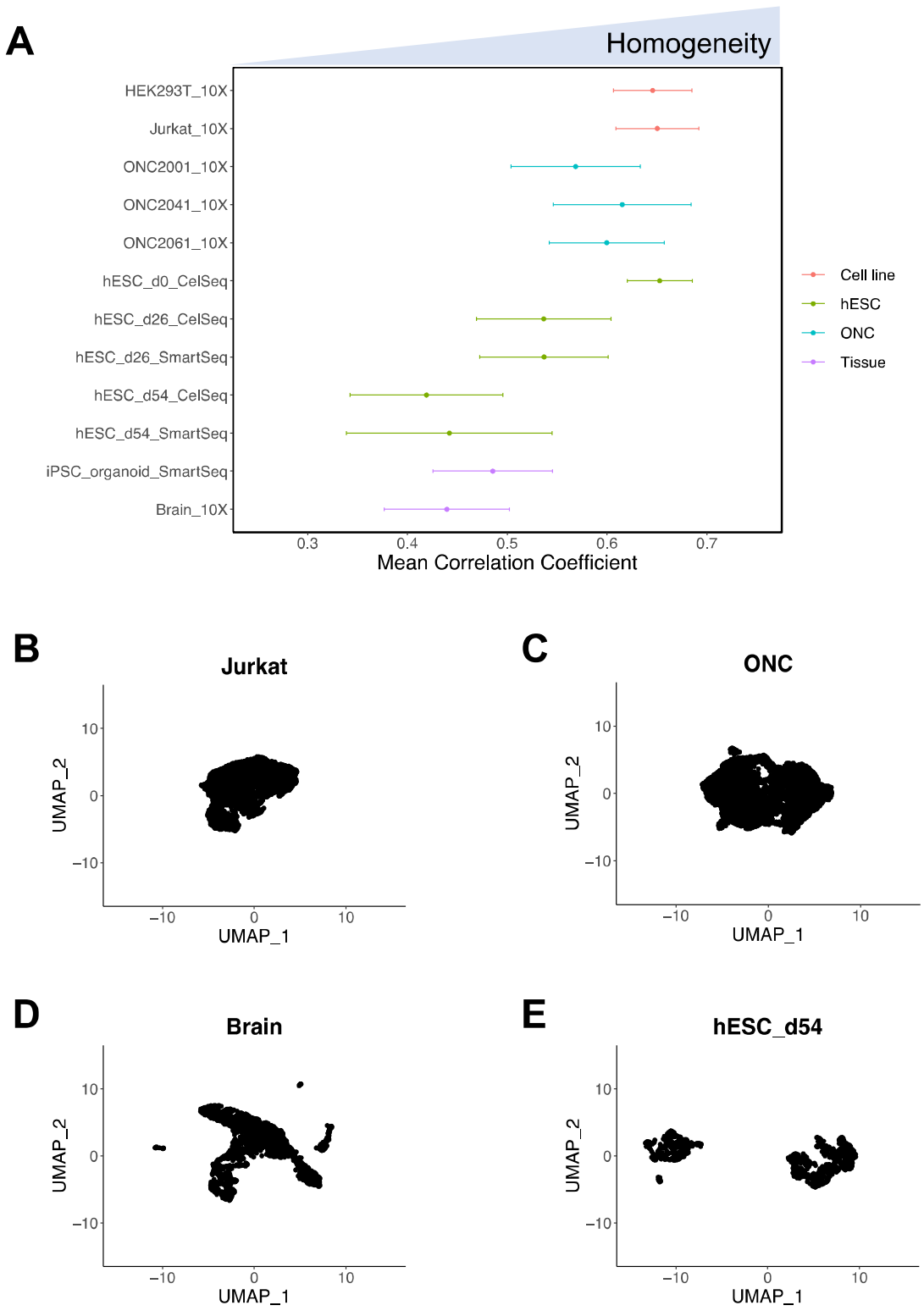
A
Homogeneity
HEK293T_10X
Jurkat_10X
ONC2001_10X
ONC2041_10X
ONC2061_10X
hESC_d0_CelSeq
hESC_d26_CelSeq
hESC_d26_SmartSeq
hESC_d54_CelSeq
hESC_d54_SmartSeq
iPSC_organoid_SmartSeq
Brain_10X
0.3
0.4
0.5
0.6
0.7
Mean Correlation Coefficient
Cell line
hESC
ONC
Tissue
B
Jurkat
C
ONC
D
Brain
E
hESC_d54
UMAP_1
UMAP_2
10
0
−10

Figure 2.

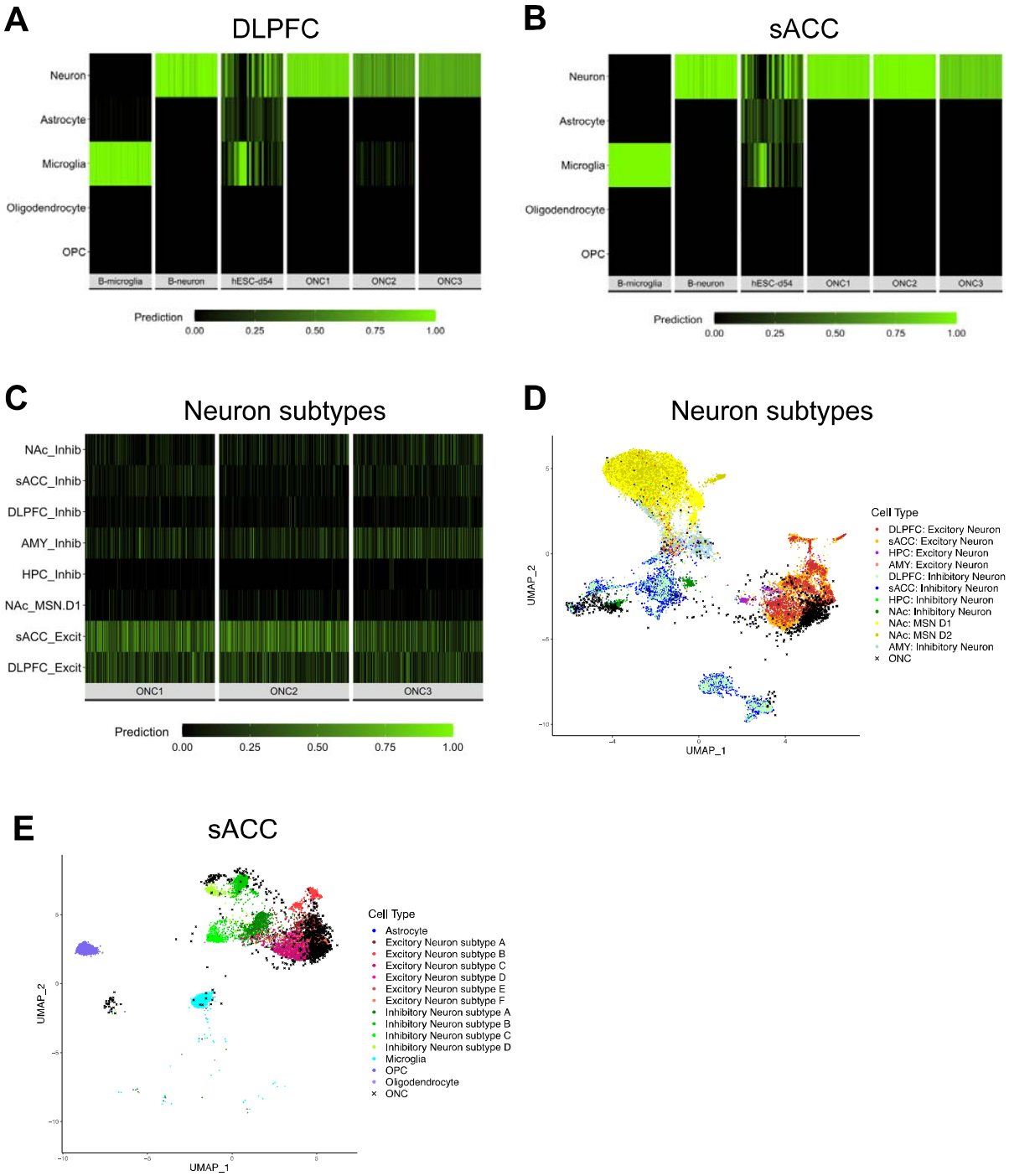
A
DLPFC
Neuron
Astrocyte
Microglia
Oligodendrocyte
OPC
B-microglia
B-neuron
hESC-d54
ONC1
ONC2
ONC3
Prediction
0.00
0.25
0.50
0.75
1.00
B
sACC
C
Neuron subtypes
NAc_Inhib
sACC_Inhib
DLPFC_Inhib
AMY_Inhib
HPC_Inhib
NAc_MSN.D1
sACC_Excit
DLPFC_Excit
D
UMAP_1
UMAP_2
Cell Type
DLPFC: Excitory Neuron
sACC: Excitory Neuron
HPC: Excitory Neuron
AMY: Excitory Neuron
DLPFC: Inhibitory Neuron
sACC: Inhibitory Neuron
HPC: Inhibitory Neuron
NAc: Inhibitory Neuron
NAc: MSN D1
NAc: MSN D2
AMY: Inhibitory Neuron
ONC
E
Astrocyte
Excitory Neuron subtype A
Excitory Neuron subtype B
Excitory Neuron subtype C
Excitory Neuron subtype D
Excitory Neuron subtype E
Excitory Neuron subtype F
Inhibitory Neuron subtype A
Inhibitory Neuron subtype B
Inhibitory Neuron subtype C
Inhibitory Neuron subtype D
Microglia
OPC
Oligodendrocyte
ONC